

- 1 **Assessment of N95 respirator decontamination and re-use for SARS-CoV-2**
- 2 Robert J. Fischer¹, Dylan H. Morris², Neeltje van Doremalen¹, Shanda Sarchette¹, M. Jeremiah Matson¹
- 3 Trenton Bushmaker¹, Claude Kwe Yinda¹, Stephanie N. Seifert¹, Amandine Gamble³, Brandi N.
- 4 Williamson¹, Seth D. Judson⁴, Emmie de Wit¹, James O. Lloyd-Smith³, Vincent J. Munster¹
- 5
- 6 1. National Institute of Allergy and Infectious Diseases, Hamilton, MT
- 7 2. Princeton University, Princeton, NJ
- 8 3. University of California, Los Angeles, Los Angeles, CA
- 9 4. University of Washington, Seattle, WA

10 The unprecedented pandemic of COVID-19 has created worldwide shortages of personal protective
11 equipment, in particular respiratory protection such as N95 respirators¹. SARS-CoV-2 transmission is
12 frequently occurring in hospital settings, with numerous reported cases of nosocomial transmission
13 highlighting the vulnerability of healthcare workers²⁻⁴. In general, N95 respirators are designed for single
14 use prior to disposal. Several groups have addressed the potential for re-use of N95 respirators from a
15 mechanical or from a decontamination perspective (for a full literature overview see Supplementary
16 Appendix).

17
18 Here, we analyzed four different decontamination methods – UV radiation (260 – 285 nm), 70°C heat,
19 70% ethanol and vaporized hydrogen peroxide (VHP) – for their ability to reduce contamination with
20 infectious SARS-CoV-2 and their effect on N95 respirator function. For each of the decontamination
21 methods, we compared the inactivation rate of SARS-CoV-2 on N95 filter fabric to that on stainless steel,
22 and we used quantitative fit testing to measure the filtration performance of the N95 respirators after each
23 decontamination run and 2 hours of wear, for three consecutive decontamination and wear sessions (see
24 Appendix). Vaporized hydrogen peroxide and ethanol yielded extremely rapid inactivation both on N95
25 and on stainless steel (Figure 1A). UV inactivated SARS-CoV-2 rapidly from steel but more slowly on
26 N95 fabric, likely due its porous nature. Heat caused more rapid inactivation on N95 than on steel;
27 inactivation rates on N95 were comparable to UV.

28
29 Quantitative fit tests showed that the filtration performance of the N95 respirator was not markedly
30 reduced after a single decontamination for any of the four decontamination methods (Figure 1B).
31 Subsequent rounds of decontamination caused sharp drops in filtration performance of the ethanol-treated
32 masks, and to a slightly lesser degree, the heat-treated masks. The VHP- and UV-treated masks retained
33 comparable filtration performance to the control group after two rounds of decontamination, and
34 maintained acceptable performance after three rounds.

35

36 Taken together, our findings show that VHP treatment exhibits the best combination of rapid inactivation
37 of SARS-CoV-2 and preservation of N95 respirator integrity, under the experimental conditions used here
38 (Figure 1C). UV radiation kills the virus more slowly and preserves comparable respirator function. 70°C
39 dry heat kills with similar speed and is likely to maintain acceptable fit scores for two rounds of
40 decontamination. Ethanol decontamination is not recommended due to loss of N95 integrity, echoing
41 earlier findings⁵.

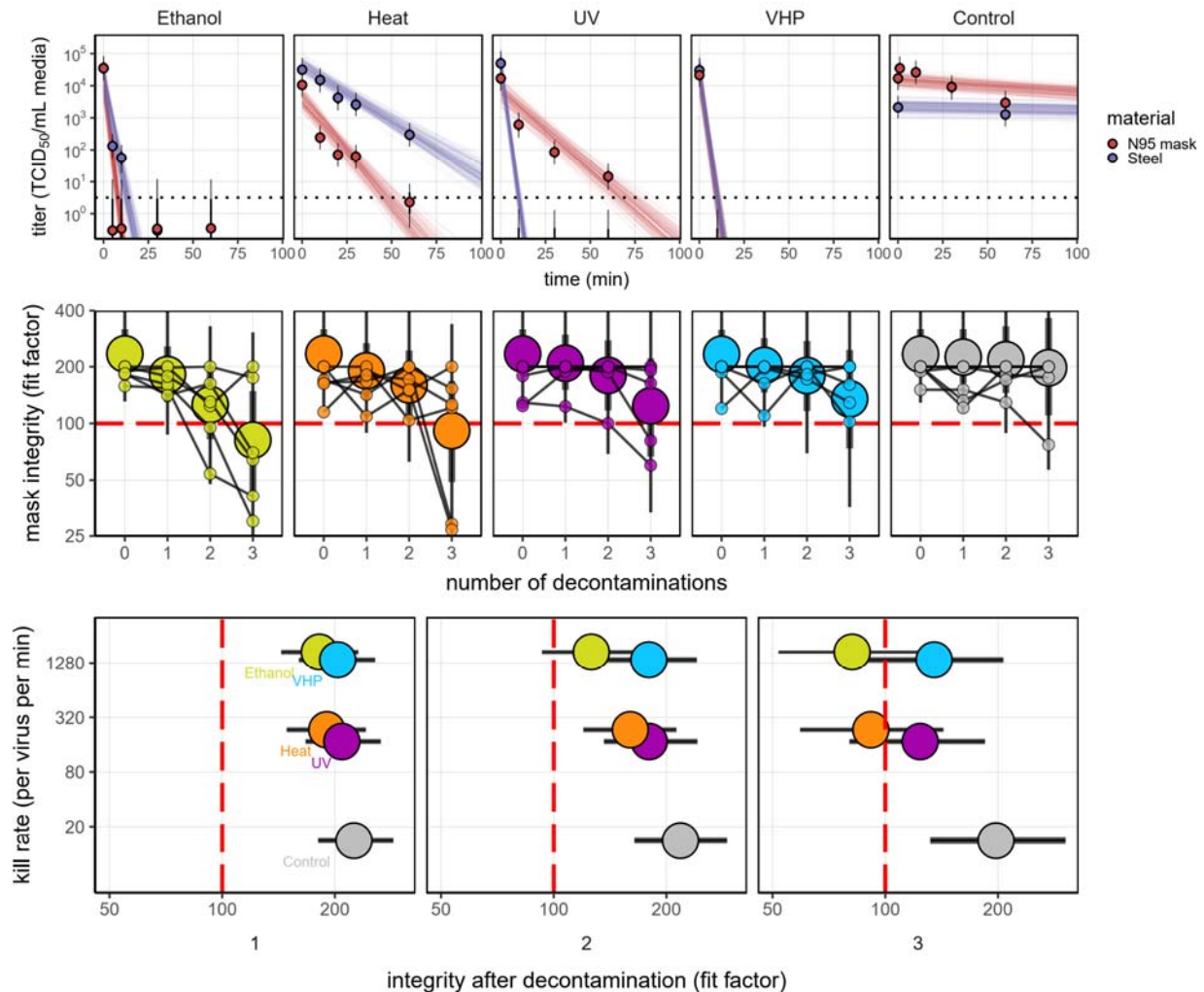
42

43 All treatments, particularly UV and dry heat, should be conducted for long enough to ensure that a
44 sufficient reduction in virus concentration has been achieved. The degree of required reduction will
45 depend upon the degree of initial virus contamination. Policymakers can use our estimated decay rates
46 together with estimates of degree of real-world contamination to choose appropriate treatment durations
47 (see Appendix).

48

49 Our results indicate that N95 respirators can be decontaminated and re-used in times of shortage for up to
50 three times for UV and HPV, and up to two times for dry heat. However, utmost care should be given to
51 ensure the proper functioning of the N95 respirator after each decontamination using readily available
52 qualitative fit testing tools and to ensure that treatments are carried out for sufficient time to achieve
53 desired risk-reduction.

54



55

56 **Figure 1.** Decontamination of SARS-CoV-2 by four different methods. **A)** SARS-CoV-2 on N95 fabric
57 and stainless steel surface was exposed to UV, 70 °C dry heat, 70% ethanol and vaporized hydrogen
58 peroxide (VHP). 50 μ l of 10⁵ TCID₅₀/mL of SARS-CoV was applied on N95 and stainless steel (SS).
59 Samples were collected at indicted timepoints post exposure to the decontamination method for UV, heat
60 and ethanol and after 10 minutes for VHP. Viable virus titer is shown in TCID₅₀/mL media on a
61 logarithmic scale. All samples were quantified by end-point titration on Vero E6 cells. Plots show
62 estimated mean across three replicates (dots and bars show the posterior median estimate of this mean and
63 the posterior inter-quartile range, or IQR). Lines show predicted decay of virus titer over time (lines; 50
64 random draws per replicate from the joint posterior distribution of the exponential decay rate, i.e. negative

65 of the slope, and intercept, i.e. initial virus titer). Black dashed line shows maximum likelihood estimate
66 titer at the Limit of Detection (LOD) of the assay: $10^{0.5}$ TCID₅₀/mL media. **B)** Mask integrity.
67 Quantitative fit testing results for all the decontamination methods after decontamination and 2 hours of
68 wear, for three consecutive runs. Data from six individual replicates (small dots) for each treatment are
69 shown in addition to the predicted median and IQR (large dots and bars respectively) fit factor. Fit factors
70 are a measure of filtration performance: the ratio of the concentration of particles outside the mask to the
71 concentration inside. The measurement machine reports value up to 200. A minimal fit factor of 100 (red
72 dashed line) is required for a mask to pass a fit test. **C)** SARS-CoV-2 decontamination performance. Kill
73 rate (y-axis), versus mask integrity after decontamination (x-axis; bar length represents IQR). The three
74 panels report mask integrity after one, two or three decontamination cycles.

75

76 **References**

- 77 1. Health C for D and R. N95 Respirators and Surgical Masks (Face Masks). FDA [Internet] 2020 [cited
78 2020 Apr 10]; Available from: [https://www.fda.gov/medical-devices/personal-protective-equipment-](https://www.fda.gov/medical-devices/personal-protective-equipment-infection-control/n95-respirators-and-surgical-masks-face-masks)
79 [infection-control/n95-respirators-and-surgical-masks-face-masks](https://www.fda.gov/medical-devices/personal-protective-equipment-infection-control/n95-respirators-and-surgical-masks-face-masks)
- 80 2. McMichael TM, Currie DW, Clark S, et al. Epidemiology of Covid-19 in a Long-Term Care Facility
81 in King County, Washington. *New England Journal of Medicine* 2020; in press.
- 82 3. Wu Z, McGoogan JM. Characteristics of and Important Lessons From the Coronavirus Disease 2019
83 (COVID-19) Outbreak in China: Summary of a Report of 72 314 Cases From the Chinese Center for
84 Disease Control and Prevention. *JAMA* 2020;323(13):1239–42.
- 85 4. Livingston E, Bucher K. Coronavirus Disease 2019 (COVID-19) in Italy. *JAMA* [Internet] 2020
86 [cited 2020 Apr 10]; Available from: <https://jamanetwork.com/journals/jama/fullarticle/2763401>
- 87 5. Liao L, Xiao W, Yu X, Wang H, Zhao M, Wang Q. Can N95 facial masks be used after disinfection?
88 And for how many times? [Internet]. Stanford University and 4C Air, Inc; 2020 [cited 2020 Apr 10].
89 Available from: <https://stanfordmedicine.app.box.com/v/covid19-PPE-1-2>

90

91

92

93

94

95	Table of contents:	page 1
96	Supplemental methods	page 2
97	Supplemental table	page 9
98	Supplemental references	page 9
99	Code and data availability	page 10
100	Acknowledgements	page 10

101 **Supplemental methods**

102 Short literature review:

103 The COVID-19 pandemic has highlighted the necessity for large-scale decontamination procedures for
104 PPE, in particular N95 respirator masks¹. SARS-CoV-2 has frequently been detected on PPE of
105 healthcare workers². The environmental stability of SARS-CoV-2 underscores the need for rapid and
106 effective decontamination methods³. Extensive literature is available for decontamination procedures for
107 N95 respirators, using either bacterial spore inactivation tests, bacteria or respiratory viruses (e.g.
108 influenza A virus)⁴⁻¹¹. Effective inactivation methods for these pathogens and surrogates include UV,
109 ethylene oxide, vaporized hydrogen peroxide, gamma irradiation, ozone and dry heat^{4,6,8,10-13}. The
110 filtration efficiency and N95 respirator fit has typically been less well explored, but suggest that both
111 filtration efficiency and N95 respirator fit can be affected by the decontamination method used^{12,14}. It will
112 therefore be critical that FDA, CDC and OSHA guidelines with regards to fit testing, seal check and
113 respirator re-use are followed^{4,15-18}.

114 ***Laboratory experiments***

115 Viruses and titration

116 HCoV-19 nCoV-WA1-2020 (MN985325.1) was the SARS-CoV-2 strain used in our comparison¹⁹.
117 Virus was quantified by end-point titration on Vero E6 cells as described previously²⁰. Virus titrations
118 were performed by end-point titration in Vero E6 cells. Cells were inoculated with 10-fold serial dilutions
119 in four-fold of samples taken from N95 mask and stainless steel surfaces (see below). One hour after
120 inoculation of cells, the inoculum was removed and replaced with 100 μ l (virus titration) DMEM (Sigma-
121 Aldrich) supplemented with 2% fetal bovine serum, 1 mM L-glutamine, 50 U/ml penicillin and 50 μ g/ml
122 streptomycin. Six days after inoculation, cytopathogenic effect was scored and the TCID₅₀ was calculated
123 (see below). Wells presenting cytopathogenic effects due to media toxicity (e.g., due to the presence of
124 ethanol or hydrogen peroxide) rather than viral infection were removed from the titer inference procedure.

125 N95 and stainless steel surface

126 N95 material discs were made by punching 9/16" (15 mm) fabric discs from N95 respirators,
127 AOSafety N9504C respirators (Aearo Company Southbridge, MA). The stainless steel 304 alloy discs
128 were purchased from Metal Remnants (<https://metalremnants.com/>) as described previously. 50 μ L of
129 SARS-CoV-2 was spotted onto each disc. A 0 time-point measurement was taken prior to exposing the
130 discs to the disinfection treatment. At each sampling time-point, discs were rinsed 5 times by passing the
131 medium over the stainless steel or through the N95 disc. The medium was transferred to a vial and frozen
132 at -80°C until titration. All experimental conditions were performed in triplicate.

133 Decontamination methods

134 *Ultraviolet light.* Plates with fabric and steel discs were placed under an LED high power UV germicidal
135 lamp (effective UV wavelength 260-285nm) without the titanium mesh plate (LEDi2, Houston, Tx) 50
136 cm from the UV source. At 50 cm the UVAB power was measured at 5 μ W/cm² using a General UVAB
137 digital light meter (General Tools and Instruments New York, NY). Plates were removed at 10, 30 and 60
138 minutes and 1 mL of cell culture medium added.

139 *Heat treatment.* Plates with fabric and steel discs were placed in a 70°C oven. Plates were removed at 10,
140 20, 30 and 60 minutes and 1 mL of cell culture medium added.

141 *70% ethanol.* Fabric and steel discs were placed into the wells of one 24 well plate per time-point and
142 sprayed with 70% ethanol to saturation. The plate was tipped to near vertical and 5 passes of ethanol were
143 sprayed onto the discs from approximately 10 cm. After 10 minutes,, 1 mL of cell culture medium was
144 added.

145 *Vaporized hydrogen peroxide (VHP).* Plates with fabric and steel discs were placed into a Panasonic
146 MCO-19AIC-PT (PHC Corp. of North America Wood Dale, IL) incubator with VHP generation
147 capabilities and exposed to hydrogen peroxide (approximately 1000 ppm). The exposure to VHP was 10
148 minutes, after the inactivation of the hydrogen peroxide, the plate was removed and 1 mL of cell culture
149 medium was added.

150 *Control.* Plates with fabric and steel discs and steel plates were maintained at 21-23°C and 40% relative
151 humidity for up to four days. After the designated time-points, 1 mL of cell culture medium was added.

152 N95 mask integrity testing

153 N95 Mask (3M™ Aura™ Particulate Respirator 9211+/37193) integrity testing after 2 hours of wear
154 and decontamination, for three consecutive rounds, was performed for a total of 6 times for each
155 decontamination condition and control condition. Masks were worn by subjects and integrity was
156 quantitatively determined using the Portacount Respirator fit tester (TSI, 8038) with the N95 companion
157 component, following the modified ambient aerosol condensation nuclei counter quantitative fit test
158 protocol approved by the OSHA (Occupational Safety and Health Administration, 2012). Subjects were
159 asked to bend over for 40 seconds, talk for 50 seconds, move head from side-to-side for 50 seconds, and
160 move head up-and-down for 50 seconds whilst aerosols on inside and outside of mask were measured. By
161 convention, this fit test is passed when the final score is ≥ 100 . For the N95 integrity testing, a Honeywell
162 Mistmate humidifier (cat#HUL520B) was used for particle generation.

163 *Statistical analyses*

164 In the model notation that follows, the symbol \sim denotes that a random variable is distributed
165 according to the given distribution. Normal distributions are parametrized as Normal(mean, standard
166 deviation). Positive-constrained normal distributions (“Half-Normal”) are parametrized as Half-
167 Normal(mode, standard deviation). Normal distributions truncated to the interval [0, 1] are parameterized
168 as TruncNormal(mode, standard deviation).

169 We use $\langle \text{Distribution Name} \rangle \text{CDF}(x \mid \text{parameters})$ and $\langle \text{Distribution Name} \rangle \text{CCDF}$ to denote the
170 cumulative distribution function and complementary cumulative distribution functions of a probability
171 distribution, respectively. So for example $\text{NormalCDF}(5 \mid 0, 1)$ is the value of the Normal(0, 1)
172 cumulative distribution function at 5.

173 We use $\text{logit}(x)$ and $\text{invlogit}(x)$ to denote the logit and inverse logit functions, respectively:

174
$$\text{logit}(x) = \ln \frac{x}{1-x} \quad (1)$$

175
$$\text{invlogit}(x) = \frac{e^x}{1 + e^x} \quad (2)$$

176 Mean titer inference

177 We inferred mean titers across sets of replicates using a Bayesian model. The \log_{10} titers v_{ijk} (the titer
178 for the sample from replicate k of timepoint j of experiment i) were assumed to be normally distributed
179 about a mean μ_{ij} with a standard deviation σ . We placed a very weakly informative normal prior on \log_{10}
180 titers μ_{ij} :

181
$$\mu_{ij} \sim \text{Normal}(3, 3) \quad (3)$$

182 We placed a weakly informative normal prior on the standard deviation:

183
$$\sigma \sim \text{Normal}(0, 0.5) \quad (4)$$

184 We then modeled individual positive and negative wells for sample ijk according to a Poisson single-
185 hit model²¹. That is, the number of virions that successfully infect cells in a given well is Poisson
186 distributed with mean:

187
$$V = \ln(2) 10^v \quad (5)$$

188 where v is the \log_{10} virus titer in TCID₅₀, where v is the \log_{10} virus titer in TCID₅₀, and the well is infected
189 if at least one virion successfully infects a cell. The value of the mean derives from the fact that our units
190 are TCID₅₀; the probability of infection at $v = 0$, i.e. 1 TCID₅₀, is equal to $1 - e^{-\ln(2) \times 1} = 0.5$.

191 Let Y_{ijkdl} be a binary variable indicating whether the l^{th} well of dilution factor d (expressed as \log_{10}
192 dilution factor) of sample ijk was positive (so $Y_{ijkdl} = 1$ if the well was positive and 0 otherwise), which
193 will occur as long as at least one virion successfully infects a cell.

194 It follows from (5) that the conditional probability of observing $Y_{ijkdl} = 1$ given a true underlying titer
195 \log_{10} titer v_{ijk} is given by:

196
$$L(Y_{ijkdl} = 1 | v_{ijk}) = 1 - e^{-\ln(2) \times 10^x} \quad (6)$$

197 Where

198
$$x = v_{ijk} - d \quad (7)$$

199 is the expected concentration, measured in \log_{10} TCID₅₀, in the dilute sample. This is simply the
200 probability that a Poisson random variable with mean $(-\ln(2) \times 10^x)$ is greater than 0. Similarly, the
201 conditional probability of observing $Y_{ijkl} = 0$ given a true underlying titer \log_{10} titer v_{ijk} is given by:

$$202 \quad L(Y_{ijkl} = 0 | v_{ijk}) = e^{-\ln(2) \times 10^x} \quad (8)$$

203 which is the probability that the Poisson random variable is 0.

204 This gives us our likelihood function, assuming independence of outcomes across wells.

205 Virus inactivation regression

206 The durations of detectability depend on the decontamination treatment but also initial inoculum and
207 sampling method, as expected. We therefore estimated the decay rates of viable virus titers using a
208 Bayesian regression analogous to that used in van Doremalen et al., 2020³. This modeling approach
209 allowed us to account for differences in initial inoculum levels across replicates as well as other sources
210 of experimental noise. The model yields estimates of posterior distributions of viral decay rates and half-
211 lives in the various experimental conditions – that is, estimates of the range of plausible values for these
212 parameters given our data, with an estimate of the overall uncertainty²².

213 Our data consist of 10 experimental conditions: 2 materials (N95 masks and stainless steel) by 5
214 treatments (no treatment, ethanol, heat, UV and VHP). Each has three replicates, and multiple time-points
215 for each replicate. We analyze the two materials separately. For each, we denote by Y_{ijkl} the positive or
216 negative status (see above) for well l which has dilution d for the titer v_{ijk} from experimental condition i
217 during replicate j at time-point k .

218 We model each replicate j for experimental condition i as starting with some true initial \log_{10} titer
219 $v_{ij}(0) = v_{ij0}$. We assume that viruses in experimental condition i decay exponentially at a rate λ_i over time t .
220 It follows that:

$$221 \quad v_{ij}(t) = v_{ij0} - \lambda_i t \quad (9)$$

222 We use the direct-from-well data likelihood function described above, except that now instead of
223 estimating titer distribution about a shared mean μ_{ij} we estimate λ_i under the assumptions that our
224 observed well data Y_{ijkl} reflect the titers $v_{ij}(t)$.

225 *Regression prior distributions*

226 We place a weakly informative Normal prior distribution on the initial \log_{10} titers v_{ij0} to rule out
227 implausibly large or small values (e.g. in this case undetectable \log_{10} titers or \log_{10} titers much higher than
228 the deposited concentration), while allowing the data to determine estimates within plausible ranges:

$$229 \quad v_{ij0} \sim \text{Normal}(4.5, 2) \quad (10)$$

230 We placed a weakly informative Half-Normal prior on the exponential decay rates λ_i :

$$231 \quad \lambda_i \sim \text{Half-Normal}(0.5, 4) \quad (11)$$

232 Our plated samples were of volume 0.1 mL, so inferred titers were incremented by 1 to convert to
233 units of \log_{10} TCID₅₀/mL.

234 Mask integrity estimation

235 To quantify the decay of mask integrity after repeated decontamination, we used a logit-linear spline
236 Bayesian regression to estimate the rate of degradation of mask fit factors over time, accounting for the
237 fact that fit factors are interval-censored ratios. Fit factors are defined as the ratio of exterior
238 concentration to interior concentration of a test aerosol. They are reported to the nearest integer, up to a
239 maximum readout of 200, but arbitrarily large true fit factors are possible as the mask performance
240 approaches perfect filtration.

241 We had 6 replicate masks j for each of 5 treatments i (no decontamination, ethanol, heat, UV and
242 VHP). Each mask j was assessed for fit factor at 4 time-points k : before decontamination, and then after 1,

243 2, and 3 decontamination cycles. We label the control treatment $i = 0$. So we denote by F_{ijk} the fit factor
244 for the j^{th} mask from the i^{th} treatment after k decontaminations (with $k = 0$ for the initial value).

245 We first converted fit factors F_{ijk} to the equivalent observed filtration rate Y_{ijk} by:

246
$$Y = 1 - 1/F \quad (12)$$

247 *Observation model and likelihood function*

248 We modeled the censored observation process as follows. $\text{logit}(Y_{ijk})$ values are observed with
249 Gaussian error about the true filtration $\text{logit}(p_{ijk})$, with an unknown standard deviation σ_o , and then
250 converted to fit factors, which are then censored:

$$251 \quad \text{logit}(Y_{ijk}) \sim \text{Normal}(\text{logit}(p_{ijk}), \sigma_o) \quad (13)$$

252 Because our reported fit factors are known to be within integer values and right-censored at 200, for
253 $F_{ijk} \geq 200$ we have a conditional probability of observing the data given the parameters of

$$254 \quad L(F_{ijk} | p_{ijk}, \sigma_o) = \text{NormalCCDF}(\text{logit}(1 - 1/200) | \text{logit}(p_{ijk}) \sigma_o) \quad (14)$$

255 That is, we calculate the probability of observing a value of F greater than or equal to 200 (equivalent a
256 value of Y greater than or equal to $1 - 1/200$), given our parameters.

257 For $1.5 \leq F_{ijk} < 200$, we first calculate the upper and lower bounds of our observation $Y^+_{ijk} = 1 - 1 /$
258 $(F_{ijk} - 0.5)$ and $Y^-_{ijk} = 1 - 1 / (F_{ijk} - 0.5)$. Then:

$$259 \quad L(F_{ijk} | p_{ijk}, \sigma_o) = \text{NormalCDF}(\text{logit}(Y^+_{ijk}) | \text{logit}(p_{ijk}) \sigma_o) - \\ 260 \quad \text{NormalCDF}(\text{logit}(Y^-_{ijk}) | \text{logit}(p_{ijk}) \sigma_o) \quad (15)$$

261 That is, we calculate the probability of observing a value between Y^+_{ijk} and Y^-_{ijk} , given our parameters.

262 *Decay model*

263 We assumed that each mask had some true initial filtration rate p_{ij0} . We assumed that these were
264 logit-normally distributed about some unknown mean mask initial filtration rate p_{avg} with a standard
265 deviation σ_p , that is:

$$266 \quad \text{logit}(p_{ij0}) \sim \text{Normal}(\text{logit}(p_{avg}), \sigma_p) \quad (16)$$

267 We then assumed that the logit of the filtration rate, $\text{logit}(p_{ijk})$, decreased after each decontamination
268 by a quantity $d_{0k} + d_{ik}$, where d_{0k} is natural degradation during the k^{th} trial in the absence of

269 decontamination (i.e. the degradation rate in the control treatment, $i = 0$), and d_{ik} is the additional
270 degrading effect of the k^{th} decontamination treatment of type $i > 0$). So for $k = 1, 2, 3$ and $i > 0$:

$$271 \quad \text{logit}(p_{ijk}) = \text{logit}(p_{ij(k-1)}) - (d_{0k} + d_{ik}) + \varepsilon_{ijk} \quad (17)$$

272 where ε_{ijk} is a normally-distributed error term with an inferred standard deviation σ_ε :

$$273 \quad \varepsilon_{ijk} \sim \text{Normal}(0, \sigma_\varepsilon) \quad (18)$$

274 And for the control $i = 0$:

$$275 \quad \text{logit}(p_{0jk}) = \text{logit}(p_{0j(k-1)}) - d_{0k} + \varepsilon_{0jk} \quad (19)$$

276 *Model prior distributions*

277 We placed a weakly informative Half-Normal prior on the control degradation rate d_0 :

$$278 \quad d_0 \sim \text{Half-Normal}(0, 0.5) \quad (20)$$

279 We placed a weakly informative Half-Normal prior on the non-control degradation rates d_i , $i > 0$:

$$280 \quad d_i \sim \text{Half-Normal}(0.25, 0.5) \quad (21)$$

281 reflecting the conservative assumption that decontamination should degrade the mask at least somewhat.

282 We placed a Truncated Normal prior on the mean initial filtration p_{avg} :

$$283 \quad p_{avg} \sim \text{TruncNormal}(0.995, 0.02) \quad (22)$$

284 The mode of 0.995 corresponds to the maximum measurable fit factor of 200. The standard deviation of
285 0.02 leaves it plausible that some masks could start near or below the minimum acceptable threshold fit
286 factor of 100, which corresponds to a p of 0.99.

287 We placed weakly informative Half-Normal priors on the logit-space standard deviations σ_p , σ_e , and
288 σ_o . σ_p reflects variation in individual masks' initial filtration about p_{avg} . σ_e reflects variation in mask's true
289 degree of degradation between decontaminations about the expected decay, and σ_o reflects noise in the
290 observation process.

$$291 \quad \sigma_p, \sigma_e, \sigma_o \sim \text{Half-Normal}(0, 0.5) \quad (23)$$

292 We chose a standard deviation of 0.5 for the priors because a standard deviation of 1.5 (i.e. 3 σ in the
293 prior) in logit space corresponds to probability values being uniformly distributed between 0 and 1; we
294 therefore wish to tell our model not to use larger standard deviations, as these squash all p_{ijk} to one of two
295 modes, one at 0 and one at 1²³.

296 Markov Chain Monte Carlo Methods

297 For all Bayesian models, we drew posterior samples using Stan (Stan Core Team 2018), which
298 implements a No-U-Turn Sampler (a form of Markov Chain Monte Carlo), via its R interface RStan. We
299 ran four replicate chains from random initial conditions for 2000 iterations, with the first 1000 iterations
300 as a warmup/adaptation period. We saved the final 1000 iterations from each chain, giving us a total of
301 4000 posterior samples. We assessed convergence by inspecting trace plots and examining R^2 and
302 effective sample size (n_{eff}) statistics.

303

304

305

306

307 **Supplemental table**

308 Table S1. Effect of decontamination method on SARS-CoV-2 viability and N95 mask integrity.

Treatment	Material	half-life (min)			time to one thousandth (min)			time to one millionth (min)		
		median	2.5%	97.5%	median	2.5%	97.5%	median	2.5%	97.5%
Control	N95 mask	78	65.3	89.7	777	650	894	1.55e+03	1.3e+03	1.79e+03
	Steel	286	243	324	2.85e+03	2.42e+03	3.23e+03	5.7e+03	4.84e+03	6.45e+03
Ethanol	N95 mask	0.639	0.55	0.721	6.37	5.49	7.19	12.7	11	14.4
	Steel	1.06	0.888	1.23	10.6	8.85	12.2	21.2	17.7	24.5
Heat	N95 mask	4.64	3.87	5.41	46.3	38.5	53.9	92.6	77	108
	Steel	8.83	7.49	10.1	88	74.7	101	176	149	201
UV	N95 mask	6.26	5.31	7.15	62.4	52.9	71.2	125	106	142
	Steel	0.733	0.649	0.802	7.31	6.47	7.99	14.6	12.9	16
VHP	N95 mask	0.78	0.685	0.858	7.78	6.82	8.55	15.6	13.6	17.1
	Steel	0.765	0.669	0.843	7.63	6.67	8.4	15.3	13.3	16.8

309

310 **Code and data availability**

311 Code and data to reproduce the Bayesian estimation results and produce corresponding figures are

312 archived online at OSF: and available on Github:

313 **Acknowledgements**

314 We would like to thank Madison Hebner, Julia Port, Kimberly Meade-White, Irene Offei Owusu,
315 Victoria Avanzato and Lizzette Perez-Perez for excellent technical assistance. This research was
316 supported by the Intramural Research Program of the National Institute of Allergy and Infectious
317 Diseases (NIAID), National Institutes of Health (NIH). JOL-S and AG were supported by the Defense
318 Advanced Research Projects Agency DARPA PREEMPT # D18AC00031 and the UCLA AIDS Institute
319 and Charity Treks, and JOL-S was supported by the U.S. National Science Foundation (DEB-1557022),
320 the Strategic Environmental Research and Development Program (SERDP, RC□2635) of the U.S.
321 Department of Defense. Names of specific vendors, manufacturers, or products are included for public
322 health and informational purposes; inclusion does not imply endorsement of the vendors, manufacturers,
323 or products by the US Department of Health and Human Services.

324

325 **Supplemental references**

- 326 1. Ranney ML, Griffeth V, Jha AK. Critical Supply Shortages - The Need for Ventilators and
327 Personal Protective Equipment during the Covid-19 Pandemic. *N Engl J Med* 2020.
- 328 2. Ong SWX, Tan YK, Chia PY, et al. Air, Surface Environmental, and Personal Protective
329 Equipment Contamination by Severe Acute Respiratory Syndrome Coronavirus 2 (SARS-CoV-2) From a
330 Symptomatic Patient. *JAMA* 2020.
- 331 3. van Doremalen N, Bushmaker T, Morris DH, et al. Aerosol and Surface Stability of SARS-CoV-2
332 as Compared with SARS-CoV-1. *N Engl J Med* 2020.
- 333 4. Decontamination and Reuse of Filtering Facepiece Respirators
334 . 2020. (Accessed 4/5/2020, 2020, at [https://www.cdc.gov/coronavirus/2019-ncov/hcp/ppe-
335 strategy/decontamination-reuse-respirators.html](https://www.cdc.gov/coronavirus/2019-ncov/hcp/ppe-strategy/decontamination-reuse-respirators.html).)
- 336 5. Final Report for the Bioquell Hydrogen Peroxide Vapor (HPV) Decontamination for Reuse of N95
337 Respirators. 2016. at <https://www.fda.gov/media/136386/download>.)
- 338 6. Fisher EM, Shaffer RE. A method to determine the available UV-C dose for the decontamination
339 of filtering facepiece respirators. *J Appl Microbiol* 2011;110:287-95.
- 340 7. Heimbuch BK, Kinney K, Lumley AE, Harnish DA, Bergman M, Wander JD. Cleaning of filtering
341 facepiece respirators contaminated with mucin and *Staphylococcus aureus*. *Am J Infect Control*
342 2014;42:265-70.
- 343 8. Heimbuch BK, Wallace WH, Kinney K, et al. A pandemic influenza preparedness study: use of
344 energetic methods to decontaminate filtering facepiece respirators contaminated with H1N1 aerosols and
345 droplets. *Am J Infect Control* 2011;39:e1-9.
- 346 9. Lin TH, Tang FC, Hung PC, Hua ZC, Lai CY. Relative survival of *Bacillus subtilis* spores loaded
347 on filtering facepiece respirators after five decontamination methods. *Indoor Air* 2018.
- 348 10. Mills D, Harnish DA, Lawrence C, Sandoval-Powers M, Heimbuch BK. Ultraviolet germicidal
349 irradiation of influenza-contaminated N95 filtering facepiece respirators. *Am J Infect Control* 2018;46:e49-
350 e55.

- 351 11. Viscusi DJ, Bergman MS, Eimer BC, Shaffer RE. Evaluation of five decontamination methods for
352 filtering facepiece respirators. *Ann Occup Hyg* 2009;53:815-27.
- 353 12. Avilash Cramer ET, Sherryl H Yu, Mitchell Galanek, Edward Lamere, Ju Li, Rajiv Gupta, Michael
354 P Short. disposable N95 masks pass qualitative fit-test but have decreases filtration efficiency after
355 cobalt-60 gamma irradiation. *MedRxiv*.
- 356 13. Chemical Disinfectants, Guideline for Disinfection and Sterilization in Healthcare Facilities. 2008.
357 at [https://www.cdc.gov/infectioncontrol/guidelines/disinfection/disinfection-](https://www.cdc.gov/infectioncontrol/guidelines/disinfection/disinfection-methods/chemical.html#Hydrogen)
358 [methods/chemical.html#Hydrogen.](https://www.cdc.gov/infectioncontrol/guidelines/disinfection/disinfection-methods/chemical.html#Hydrogen))
- 359 14. Lin TH, Chen CC, Huang SH, Kuo CW, Lai CY, Lin WY. Filter quality of electret masks in filtering
360 14.6-594 nm aerosol particles: Effects of five decontamination methods. *PLoS One* 2017;12:e0186217.
- 361 15. N95 Respirators and Surgical Masks (Face Masks). 2020. (Accessed 4/5/2020, 2020, at
362 [https://www.fda.gov/medical-devices/personal-protective-equipment-infection-control/n95-respirators-and-](https://www.fda.gov/medical-devices/personal-protective-equipment-infection-control/n95-respirators-and-surgical-masks-face-masks)
363 [surgical-masks-face-masks.](https://www.fda.gov/medical-devices/personal-protective-equipment-infection-control/n95-respirators-and-surgical-masks-face-masks))
- 364 16. Temporary Enforcement Guidance - Healthcare Respiratory Protection Annual Fit-Testing for N95
365 Filtering Facepieces During the COVID-19 Outbreak. 2020. at [https://www.osha.gov/memos/2020-03-](https://www.osha.gov/memos/2020-03-14/temporary-enforcement-guidance-healthcare-respiratory-protection-annual-fit)
366 [14/temporary-enforcement-guidance-healthcare-respiratory-protection-annual-fit.](https://www.osha.gov/memos/2020-03-14/temporary-enforcement-guidance-healthcare-respiratory-protection-annual-fit))
- 367 17. User Seal Check Procedures (Mandatory). 2020. (Accessed April 11, 2020, at
368 [https://www.osha.gov/laws-regs/regulations/standardnumber/1910/1910.134AppB1.](https://www.osha.gov/laws-regs/regulations/standardnumber/1910/1910.134AppB1))
- 369 18. Respirator Fit Testing [WWW Document]. U. S. Dep. Labo. 2012. at
370 https://www.osha.gov/video/respiratory_protection/fittesting_transcript.html (accessed 4.10.20.)
- 371 19. Holshue ML, DeBolt C, Lindquist S, et al. First Case of 2019 Novel Coronavirus in the United
372 States. *N Engl J Med* 2020.
- 373 20. van Doremalen N, Bushmaker T, Munster VJ. Stability of Middle East respiratory syndrome
374 coronavirus (MERS-CoV) under different environmental conditions. *Euro Surveill* 2013;18.
- 375 21. Brownie C, Statt J, Bauman P, et al. Estimating viral titres in solutions with low viral loads.
376 *Biologicals* 2011;39:224-30.
- 377 22. Gelman A. Bayesian data analysis. Third edition. ed. Boca Raton: CRC Press; 2014.
- 378 23. Northrup JM, Gerber BD. A comment on priors for Bayesian occupancy models. *PLoS One*
379 2018;13:e0192819.

380

381